1971

An analog computer simulation of the flapping of a helicopter hinged main rotor blade

Edward Charles Robinson

Recommended Citation

AN ANALOG COMPUTER SIMULATION OF THE FLAPPING

OF A HELICOPTER HINGED MAIN ROTOR BLADE

BY

EDWARD CHARLES ROBINSON, 1937-

A

THESIS

submitted to the graduate faculty of

THE UNIVERSITY OF MISSOURI-ROLLA

in partial fulfillment of the requirements for the

Degree of

MASTER OF SCIENCE IN AEROSPACE ENGINEERING

Rolla, Missouri

1971

Approved by

_____ (Advisor) _____

_____

ABSTRACT

An analog computer simulation was performed on the Systron Donner SD 40/80 electronic differential analyzer consisting of one panel (SD 40) less three modules augmented by three digital logic modules for iterative operation.

The flapping equation was solved in continuous iteration for various values of blade mass and the resultant blade flapping magnitudes and harmonic coefficients were compared in computer plots of the blade tip path plane. A flap compensator was added and the result plotted. Various aerodynamic parameters of the flapping equation solution were plotted.

ACKNOWLEDGEMENTS

TABLE OF CONTENTS

LIST OF ILLUSTRATIONS

CHAPTER I

INTRODUCTION

This investigation is concerned with the analysis
of helicopter main rotor aerodynamics utilizing an
analog computer (electronic differential analyzer) to
solve the blade flapping equation. A helicopter is a
unique aircraft in that in forward flight a rotor blade,
for a portion of the cycle, is moving upwind and for the
remaining portion it is moving downwind (see Fig. 1). The
consequent increase and decrease in relative velocities
across the rotor blade results in a differential lift
around the rotor blade azimuth as well as along the
radius of the rotor blade. Some compensation must be
made for this azimuthal differential lift or the helicopter
would have a continuous moment applied to it in the roll
and pitch axes. This problem was first encountered by
Juan De La Cierva in his first experiments with the
autogyro. Cierva solved the problem by hinging the rotor
blade in the flapping (horizontal) axis so that as the
blade rose due to the increased lift, and vice versa, the
moment resulting from the varying lift was not imparted
to the aircraft itself. Another benefit of the flapping
blade was that as a result of the flapping velocity, the
relative angle of attack or the angle of the relative
wind velocity to the rotor blade chord was decreased on
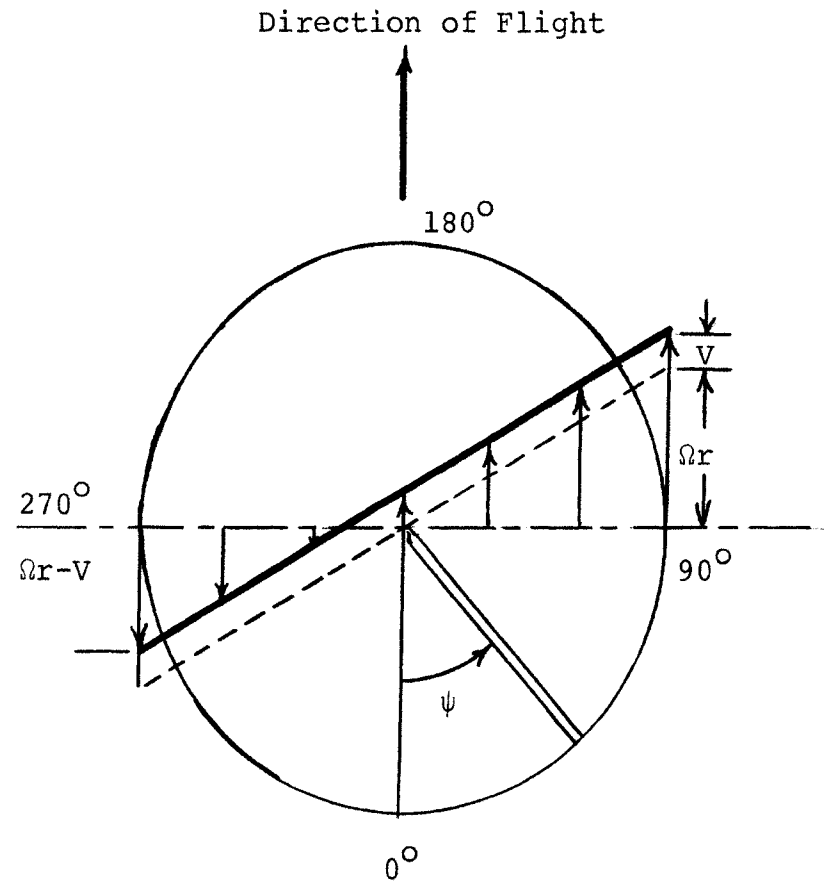
Figure 1. Velocity Distribution in Forward Flight

the advancing blade side of the aircraft and increased on the retreating blade side of the aircraft. The further result was an equalization of the lift around the blade azimuth of rotation which tended to damp the flapping oscillation of the blade.

It is this blade flapping which was modeled and studied in this thesis with continuous observation of the aerodynamic inputs to the flapping equation on the analog computer. The effect of varying blade inertial moments and flap compensation on flapping and phase angle is shown.

In summary, the purpose of the study was two fold: 1) To develop a main rotor simulation which could be programmed on the available SD 40 computer and which could be expanded as additional components are added to the SD 80 capacity of the computer, 2) To provide a medium for the author to study and experiment with the aerodynamics of the helicopter and the simulation of a portion of a helicopter flight system.

CHAPTER II

REVIEW OF LITERATURE

During the decade of the sixties, perhaps because
of the impetus given to the helicopter by the airmobile
tests of the American Army and the extensive use of the
helicopter in the Vietnam conflict, a great deal of
interest was generated in developing computerized simu-
lations of the flight of a helicopter.

In the fifties MacNeal (1958) and Hohenemser (1958)
experimented with electrical and mechanical analogies of
aerodynamic problems. In the early sixties Jones (1963,
1964) of Great Britain, utilized an analog computer to
calculate rotor blade motion. It is the original ideas
of Jones which provide the basic structure of the analog
analysis presented here. Jones (1964) presented his
results as a plot of flapping versus sin ψ without
magnitudes and simulated the effects of a stall without
detailing any specific rotor blade or helicopter. Inertial
effects and flap compensation were not considered and blade
twist and reverse flow were ignored.

In 1963 a study was conducted in the United States
for the Naval Training Device Center then at Port
Washington, New York (NAVTRADEVCEN 1205-1, 1963), to analyze
the equations of motion of Vertical/Short takeoff and
landing flight weapons system trainers and to develop an

analog and digital simulation analysis of V/STOL Aircraft.

In 1965, Electronics Associates, Inc. published a simulation of helicopter motion and avionics systems for the U.S. Army Electronic Laboratories to study the inter-action between avionics systems and the helicopter. Electronic Associates, Inc. subsequently extended their analysis, publishing in 1969 a hybrid computer program for the simulation of the U.S. Army's AHIG Cobra (ECOM 0387-F1, 1969) and the AH56 Cheyenne (ECOM 0387-F2, 1969). The latter work was also for the now U.S. Army Electronics Command. These were extensive works, modeling all inputs for a simulated flight trainer with a pilot at the con-trols. Published documents however do not show data relating to the flapping aerodynamics of the helicopter rotor and construction of the simulation requires exten-sive digital and analog equipment.

It is known that the Russians (Volodkov, 1968) have also performed analog simulations of helicopters to analyze the effects on the helicopter of the loss of por-tions of the main rotor and tail rotor blades. This work was published in the Soviet Union in Russian and is unavailable to the author.

The advantage of an analog simulation of a helicopter rotor over a digital simulation is that the analog computer can instantaneously solve the non-linear partial differential equations with variable coefficients whereas a digital

computer takes considerably more time. An electronic analog solution also can integrate along the entire radius of the blade and with rapid iterations over very small azimuth steps, thus giving a high degree of accuracy on a sufficiently flexible analog computer. This becomes particularly important when higher harmonics of bending and torsion are introduced into the problem. The small azimuth step is also necessary if the higher harmonics resulting from impulsive disturbances are to be represented and observed since they are of a transient nature. At very high tip speeds, severe non-linearities may result with very large variations of the flapping coefficients, introducing sub-harmonics as well as the higher harmonics, where the blade flapping no longer repeats itself during each revolution.

The digital simulation techniques require a steady state solution time and the large azimuth and radial steps inherent in the digital solution hinder complete observation of harmonics. The tabular form of output data from a digital simulation is not presented in the best form for observing the main features and more signi-ficant parameters which can be observed on the analog computer plots.

NAVTRADEVCEN 1205-4 (1964) specifically studied the feasibility of reduction in the number of azimuth stations which were necessary in order to reduce digital computa-tions in a helicopter rotor simulation and determined

that mean performance values of sufficient accuracy for a flight simulator could be obtained with four azimuth and three radial stations in integration, in order to reduce digital computer solution time to real time.

Schramm (1970) published for Bell Helicopter a paper on a real-time simulation of a helicopter rotor using a Hybrid Systems, Inc. SS-100 Analog/Hybrid Computer for his rotor solution. The results agreed very closely with a non-realtime Bell digital program. All aspects of the helicopter were modeled and an auto pilot trimmed the helicopter.

For a detailed and fundamental description of the aerodynamics of the helicopter the reader is referred to Gessow and Myers (1967), a text which seems to be the international standard reference text of all subsequent publications since it was originally published in 1952. It is from this text that the author draws most heavily in basic theory.

It is not the intention of the author to present a study of helicopter aerodynamics in this study, however, sufficient introduction is presented to understand the problem.

CHAPTER III

ANALYSIS OF EQUATIONS

The analysis which is presented is restricted in a sense by the size and capacity of the computer and does not pretend to be a complete model of a helicopter. A complete model would incorporate not only main rotor aerodynamics but tail rotor aerodynamics, fuselage aerodynamics, earth coordinates, pilot response, and engine response, involving extremely large and expensive digital and analog equipment. The main rotor analyzed here has been simplified by several assumptions which limit the model to a degree but which are valid under the conditions presented.

Figure 2 illustrates the helicopter blade element from which the blade flapping equation is derived. Assuming that the blade is hinged horizontally on the axis of rotation the summation of the moments about this hinge in the flapping axis is

$$\Sigma M = 0 = -\Omega^2 \sin\beta \, \cos\beta \int_0^R mr^2 dr$$

$$- \frac{d^2\beta}{dt^2} \int_0^R mr^2 dr + \int_{r_o}^R rdL \qquad (1)$$

The blade weight, being small in comparison with the other forces, is neglected in the summation of moments.
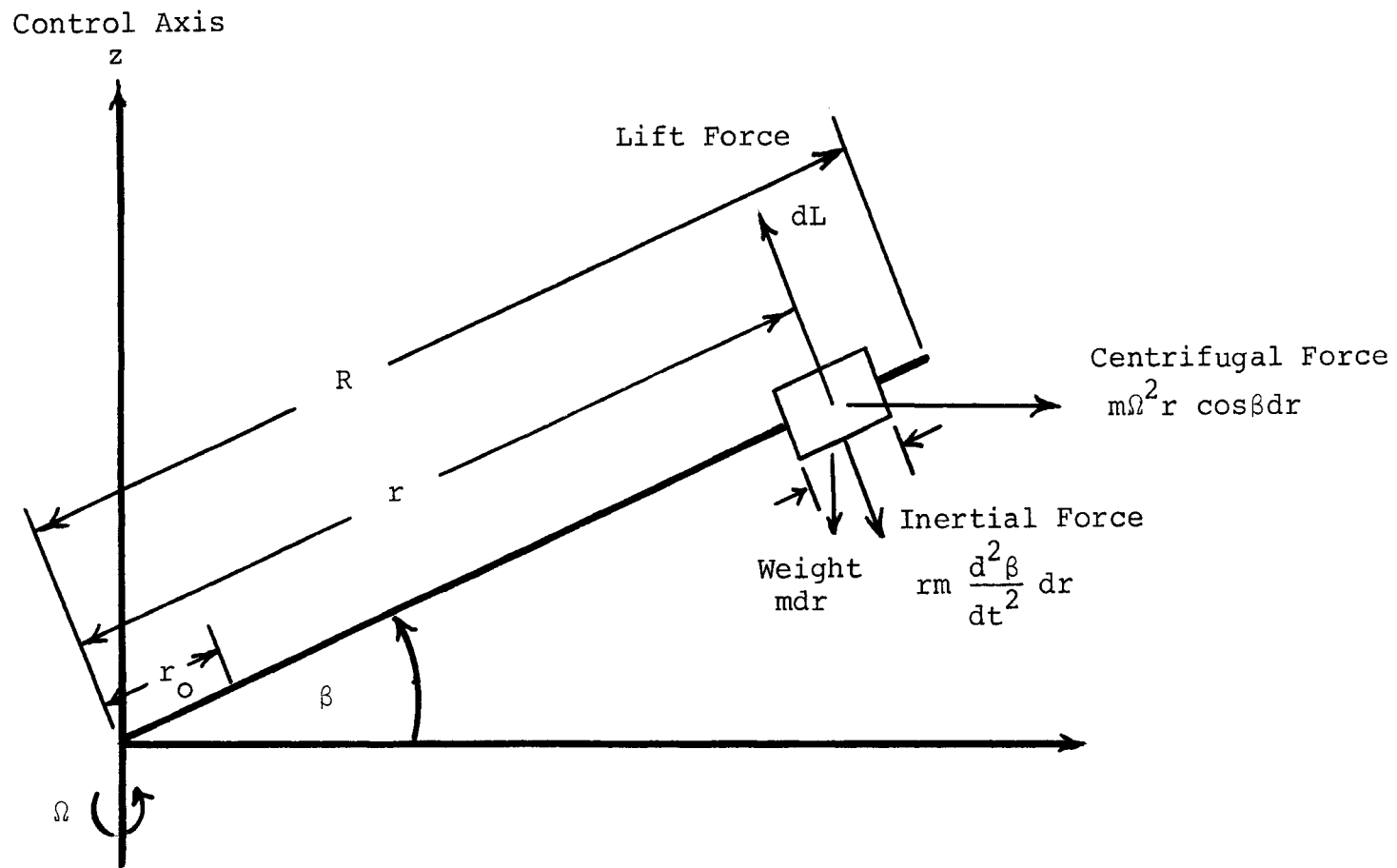
Figure 2. Blade Element Forces

The assumption is also made that β is a small angle, which is the case in a properly designed helicopter. Since

$$\int_0^R mr^2 dr = I \ ,$$

the equation resolves to

$$\left(\frac{d^2\beta}{dt^2} + \beta\Omega^2\right) I = \int_{r_o}^R rdL \tag{2}$$

Since the rotational velocity of a helicopter rotor is maintained constant either manually or by a fuel control governor, the azimuth angle of rotation

$$\psi = \Omega t \quad \text{and} \quad d\psi = \Omega dt \tag{3}$$

consequently

$$d^2\psi = \Omega^2 dt^2 \quad \text{or} \quad dt^2 = \frac{1}{\Omega^2} \ d\psi^2 . \tag{4}$$

Resolving equation (2),

$$\left(\frac{1}{\Omega^2} \frac{d^2\beta}{dt^2} + \beta\right) I \ \Omega^2 = \int_{r_o}^R rdL$$

or

$$\frac{1}{\Omega^2} \frac{d^2\beta}{dt^2} = -\beta + \frac{1}{I\Omega^2} \int_{r_o}^R rdL \tag{5}$$

Equation (5) shall be known as the flapping equation. The flapping equation can easily be solved on the analog

computer and is analogous to a mechanical single degree
of freedom spring mass system with damping and a sinusoidal
driving force discussed in Gessow and Myers (1967, pp. 156-
158). A more complete discussion of vibration of spring
mass systems of this type can be found in Thomson (1965,
pp. 51-57). The difficulty in the solution of the
flapping equation lies in solving for the unknown integral
$\int_{r_o}^{R}$ rdL. The solution of this integral requires the
greatest expenditure of computer components and the
monitoring of these circuits also enables one to gain
insight into the varying forces and velocities acting on
the rotor blade along its radius and around the rotor
azimuth of traverse. The analysis of the lifting moment
integral $\int_{r_o}^{R}$ rdL assumes a rigid blade with no bending
and neglects the small region of reverse flow which
occurs inboard on the retreating blade at speeds where the
velocity of the aircraft exceeds the rotational velocity
of the rotor blade. Neglecting this reverse flow region
has negligible effect at the tip speed ratios of most of
today's helicopters. It's primary effect is on the
coefficients of higher harmonics of flapping which are
small. Lifting forces near the hub are small due to the
low rotational velocity in this area. Blade twist is
taken into account and the lift distribution approximates
that for an ideally twisted blade described in Gessow and
Myers (1967, p. 142). The formulas used in the solution
of the lift moment integral are presented not in the

non-dimensional form commonly used but in a dimensional
form in order that these quantities can be recorded and
observed as physical quantities acting on the rotor. The
small angle assumption is made for the flapping angle β,
rotor tilt α_t and angle of inflow to the rotor disc, ϕ.

A further assumption of uniform inflow through the
rotor disc is made. This assumption is common at higher
velocities. Coriolis forces are neglected and are not
present when the blade is hinged on the axis of rotation.
Rotor blade stall has not been incorporated into the
model because of lack of components. A lift slope
potentiometer is used to determine the coefficient of
lift resulting from the resultant angle of attack and
the angle of attack is maintained within stall boundaries.
Stall can be modeled by use of a diode function generator
to construct the coefficient of lift curve versus angle
of attack α. The slope of the curve can be changed for
varying mach numbers, but for purposes of this model,
little error results in maintaining the coefficient of
lift curve at a constant slope. It is the author's con-
tention that blade stall is normally of little consequence
because most helicopters are limited in the power to
achieve a stall and will first lose engine rotational
speed due to the increased drag at high angle of attack.
Upon loss of rotor speed the collective pitch would be
lowered by the pilot or forward speed would be reduced,

thus preventing the stall.

The axis of reference will be the axis of no cyclic feathering (control axis) used by Gessow and Myers (1967, pp. 181-183). The control axis can also be described as perpendicular to the swash plate. Use of the control axis eliminates unnecessary complications in analysis of blade flapping because cyclic blade feathering is zero in this axis of reference. The computer circuit used in this study is not confined to the control axis. Use of the control axis will permit a comparison of data with the theory presented in Gessow and Myers.

From equation (5) it can be seen that

$$\beta = \frac{1}{I\Omega^2} \int_{r_o}^{R} rdL - \frac{1}{\Omega^2} \frac{d^2\beta}{dt^2} \tag{6}$$

The flapping angle β can also be expressed as a Fourier series where

$$\beta = a_o - a_1\cos\psi - b_1\sin\psi - a_2\cos2\psi - b_2\sin2\psi - a_3\cos3\psi \ldots \tag{7}$$

where all harmonics above the second have been found experimentally to be small. Consequently,

$$\frac{d\beta}{dt} = \Omega(a_1\sin\psi - b_1\cos\psi) \tag{8}$$

$$\frac{d^2\beta}{dt^2} = \Omega^2(a_1\cos\psi + b_1\sin\psi) \tag{9}$$

The relationship of equation (5) with equation (7) can now be seen as

$$a_o = \frac{1}{I\Omega^2} \int_{r_o}^{R} rdL \qquad (10)$$

where a_o is the coning angle of the blade resulting from
blade lift. Equation (10) is true only when first har-
monic flapping motion is considered.

Incorporated in a_o or

$$\frac{1}{I\Omega^2} \int_{r_o}^{R} rdL$$

is the lock number γ described in Gessow and Myers (1967,
p. 194) as the relationship between the air forces and
mass forces acting on the blade. Recall that the dimen-
sional form of the equations described later is being
used rather than the non-dimensional form when relating
γ to a_o in this study since γ is the non-dimensional
form of the Lock number. Further discussion of the Lock
number is irrelevant to this study and can be satisfied
by the reader concurrent with his interest. Suffice it
to say that the coning angle is proportional to the Lock
number, a_1 is independent of the Lock number, and that
b_1 is proportional to the coning angle. Coefficient a_1
can be described as the amplitude of a pure cosine motion
or fore and aft rotor tilt and b_1 as the amplitude
of a pure sine motion or sideward rotor tilt. The
coefficient a_o represents the coning angle of the rotor
blade. When the helicopter is hovering, $\beta = a_o$, the

coning angle. It can now be seen that a_o depends upon the magnitude of the lift (thrust) moment and the centrifugal moment, hence the Lock number.

A rotor with very heavy blades performs a nearly pure a_1 flapping motion with the coning angle, sideward tilt, and higher harmonic flapping becoming greater as the blades become lighter.

A discussion of the rotor blade angle of attack is now in order. The geometric angle of attack of the helicopter blade represents the feathering motion of the blade with respect to the plane of the blade tips and can be represented as a Fourier series where

$$\theta = \theta_o - \theta_1 \cos\psi - \theta_2 \sin\psi \ldots \tag{11}$$

Coefficient θ_1 represents the amplitude of the angle of lateral cyclic control and θ_2 represents the amplitude of the angle of longitudinal cyclic control.

Equation (11) is modified to incorporate the angle of blade twist at each radial station by adding the blade twist rate multiplied by the radial distance or $\theta_t = r\theta_r$. θ_o represents the amplitude of the angle of collective pitch. In this study, θ_o is taken as the angle of collective pitch at the inner radius in order that a radial integration from inner radius to outer radius times the negative blade twist may be subtracted from θ_o giving θ at the outer radius equal to the collective pitch at the

blade tips when no cyclic pitch is applied. The geometric
blade angle of attack is modified aerodynamically in flight,
as stated earlier, primarily by the blade flapping influence
on the angle of inflow to the rotor. Adding an angle of
inflow, ϕ, to the geometric angle of attack yields a resul-
tant angle of attack

$$\alpha = \theta_o - \theta_t - \theta_1\cos\psi - \theta_2\sin\psi + \phi \qquad (12)$$

The sign of ϕ is determined by the sign of the velocity
component perpendicular to the rotor disc, U_p. Figure 3
illustrates the effect of the perpendicular velocity U_p
and the tangential velocity U_T on the blade, where U_T
represents the velocity component parallel to the rotor
disc or swash plate (perpendicular to control axis).

Velocity components of U_T are illustrated in figure 4
where α_t, the tilt of the swash plate, is assumed to be a
small angle, thus $\cos \alpha_t = 1$. It can be easily seen from
figure 4 that

$$U_T = \Omega r + V\cos \alpha_t \sin\psi$$
$$= \Omega r + V \sin\psi \qquad (13)$$

and is given that

$$U_p = (V \sin \alpha_t + \nu)\cos\beta - r \frac{d\beta}{dt} - V \cos \alpha_t\cos\psi \sin\beta$$

$$= V \alpha_t + \nu - r \frac{d\beta}{dt} - V\beta \cos\psi \qquad (14)$$

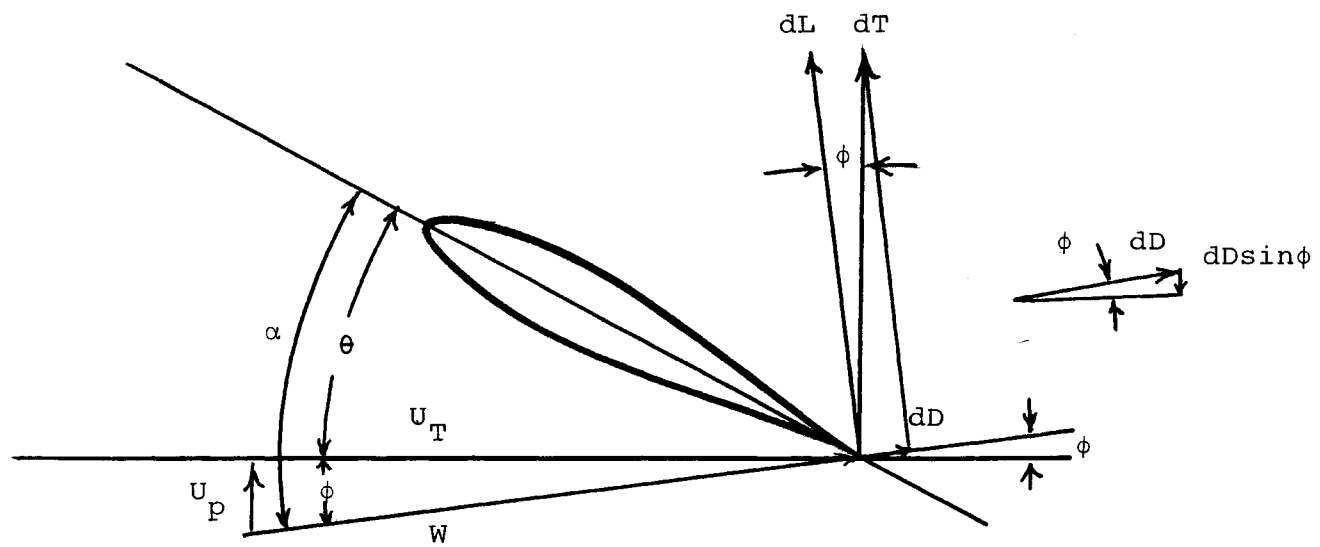Figure 3. Resultant Angle of Attack of Blade Element

Direction of Flight

Direction of
Rotation

r

Ωr

ψ

$V\cos\alpha_t \sin\psi$

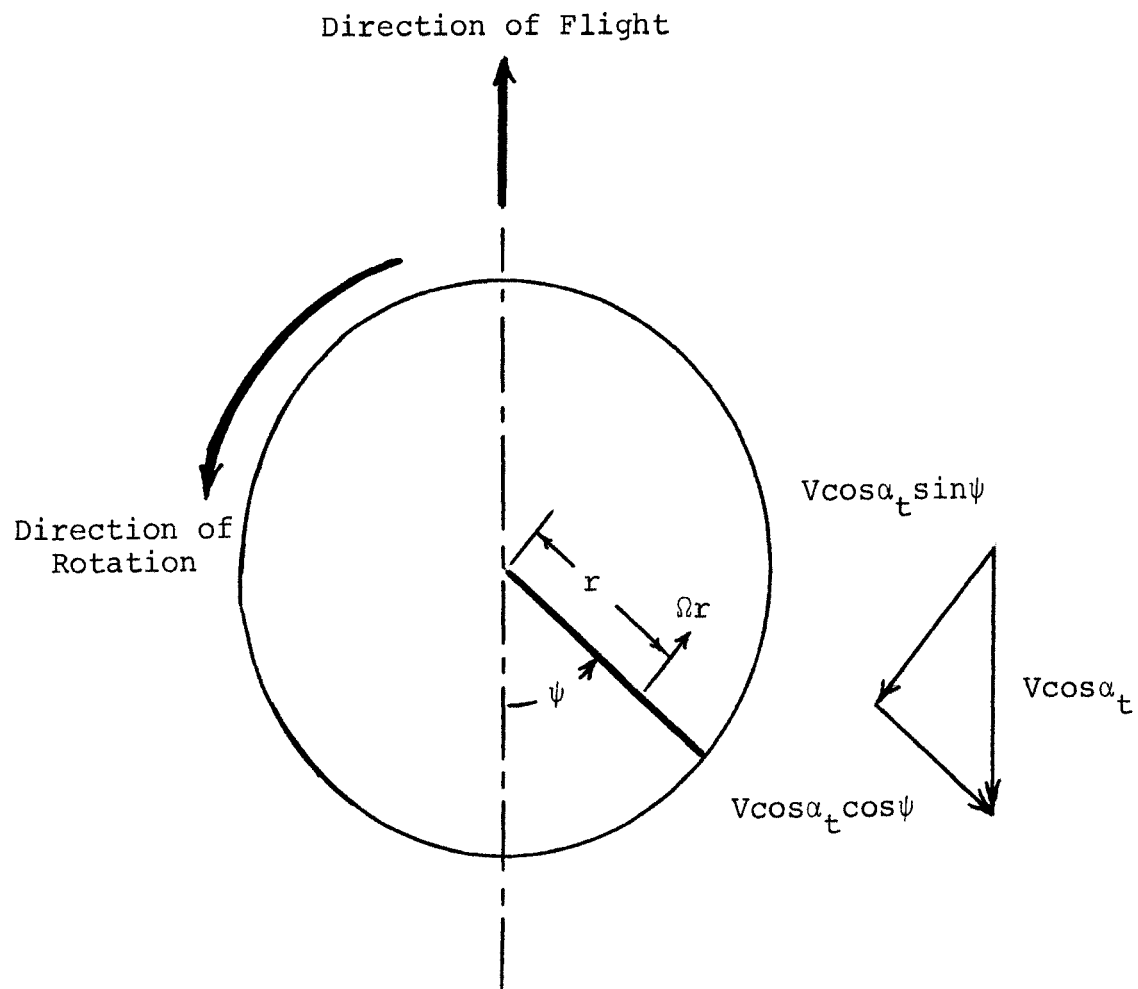$V\cos\alpha_t$

$V\cos\alpha_t \cos\psi$

Figure 4. Velocity Components Perpendicular to
Control Axis

where ν is the induced velocity. Sign convention used here for forward swash plate tilt, $-\alpha_t$, is negative as is downward induced velocity, $-\nu$.

Equation (13) and (14) are expressed in the dimensional form as explained earlier and will remain so.

Using the small angle assumption it can also be seen from figure 3 that

$$\phi = \tan^{-1} \frac{U_p}{U_T} = \frac{U_p}{U_T} . \tag{15}$$

Blade element coefficient of lift C_L is determined for the particular angle of attack, α, by multiplying by slope, a. Sufficient information is now available to solve for $\int_{r_o}^{R} rdL$ since $dL = \frac{1}{2} \rho W^2 C_L cdr$ from the blade element theory where W is the resultant velocity depicted in figure 3. The blade element lift, dL, will be considered equivalent to the blade element thrust, dT, from the small angle assumption for ϕ in figure 3 since $dT = dL\cos\phi - dD\sin\phi$, where dD and ϕ are both small.

The analog computer program for evaluating $\int_{r_o}^{R} rdL$ and for solving the flapping equation is presented in figure 5. The technique illustrated in figure 5 is to generate a rapid iteration of the ramp function r_o to R on integrator number 1 while it is in compute during switching mode A. While integrator number 1 is in compute , this in effect produces $\frac{1}{2} \rho c \ C_L W^2 dr = dL$ for every radial station in a continuous calculation. The radius generated is also used in contributing blade twist to α along the blade radius;
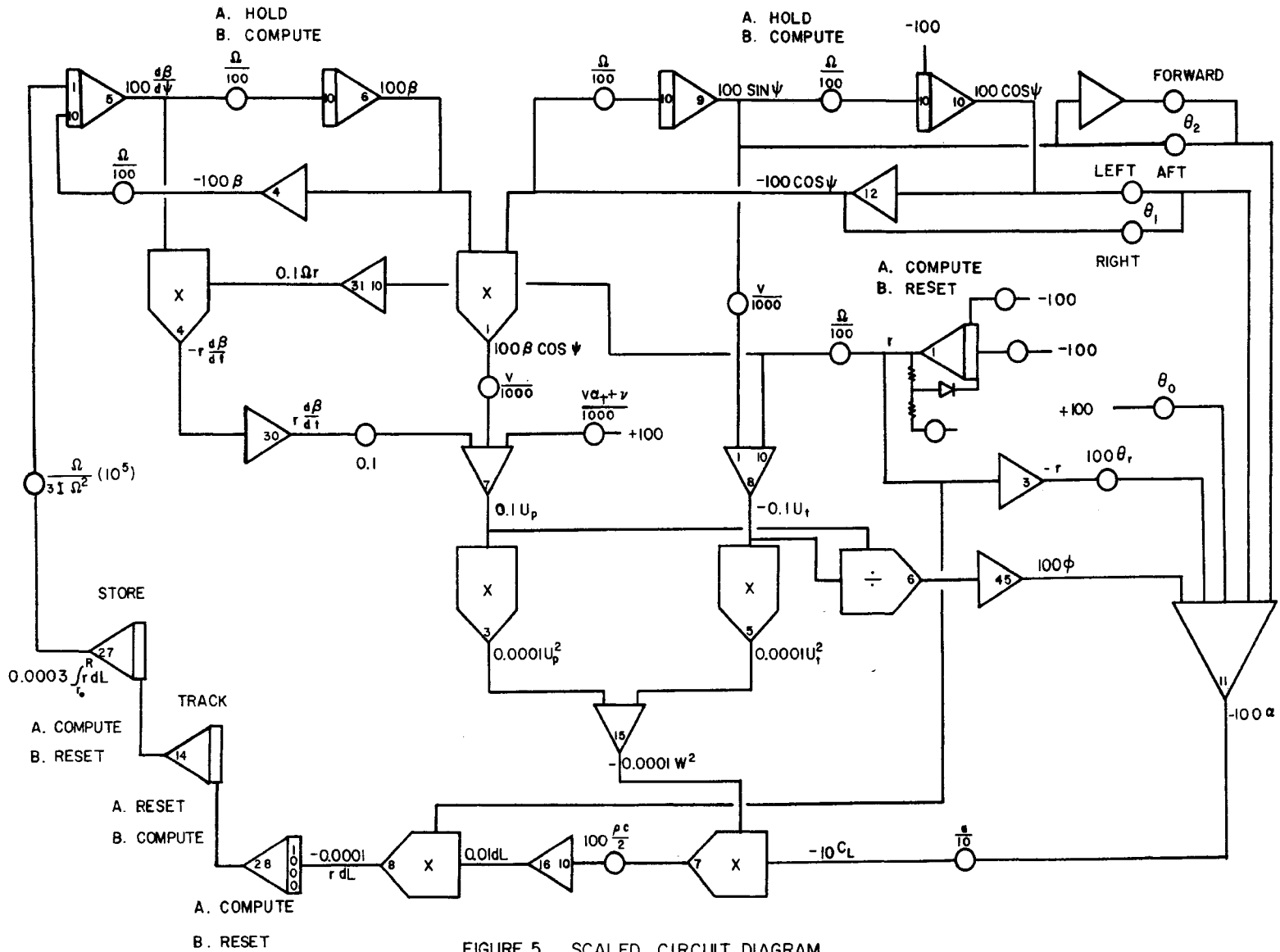
FIGURE 5. SCALED CIRCUIT DIAGRAM

in computing $r \frac{d\beta}{dt}$; and in determining rdL for integration.
While the radius is being generated $\sin\psi$ and $\cos\psi$ are in
hold and thus are constant during the radial integration
as is β and $\frac{d\beta}{d\psi}$. Integrator number 28 meanwhile is inte-
grating the indefinite integral, $\int$ rdL. The track inte-
grator, number 14, is in reset and tracking the integration
through its initial condition capacitors and the store
integrator, number 27, is in compute which allows it to
store the final value from the previous iteration. To
enable the track and store modules to hold information long
enough to pass from track to store and from store to
integrator number 5 between switching modes, a short hold
period is necessary between modes A to B, and B to A
as discussed in Gilliland (1967, p. 15-2). This feature
can be incorporated using the digital logic section to
drive the rep-op switching of the integrators. A modified
logic program from Gilliland (1967, p. 15-4) was used for
timing and switching the busses. The integrator iterative
operation (IO) patching circuits were modified from
Gilliland (1967, p. 15-3) to control the integrator modules
from the compute - reset-hold busses.

During switching mode B, integrator number 1 returns
to reset as does integrator number 27 and 28. Meanwhile
$\sin\psi$ and $\cos\psi$ procede in compute as does $\frac{d\beta}{d\psi}$ and β which is
using the definite integral from integrator 27, now in
reset. Integrator 27 has picked up the final value of
the previous iteration from integrator number 14 which is

in compute and holding. When the track and store inte-
grators are in compute they are actually holding the
value which was placed on their initial condition capa-
citors during reset. The computer next passes through
a short hold period and returns to mode A for another
iteration.

It can be seen that with rapid switching and small
impedance capacitors to shorten the time constant many
iterations of radial integration $\int_0^{2\pi} \int_{r_o}^{R} \frac{rdL}{dr} dr d\psi$ can
be accomplished during each cycle of blade rotation. The
SD 40/80 is equipped with reed switches which limit the
switching speed to an extent but the primary limitation
was in the 0.01 microfarad capacitors on the track and
store integrators and integrator number 28. It was deter-
mined that the gain of the definite integral on integrator
number 27 could not be predicted by the value of the
input resistor and feedback capacitance on integrator 28.
The switching time and some discrete values of incremental
lift, dL, were used to calculate the scale of the definite
integral on integrator number 27. To scale integrator 27,
the lift distribution for an ideally twisted blade was
taken for dL data from r_o to R to calculate the actual
discrete value of the definite integral $\int_{r_o}^{R} rdL$ at some
discrete ψ and the scale was thereby determined for contin-
uous data. Graphic illustration of switching modes for
all integrators is shown in figure 6. Jones (1964) sug-
gested that $\sin\psi$ and $\cos\psi$ be left in continuous compute

INTEGRATORS

   1, 27, 28

COMPUTE

HOLD

RESET

INTEGRATORS

   5, 6, 9, 10

COMPUTE

HOLD

RESET

INTEGRATORS

   13, 14

COMPUTE

HOLD

RESET

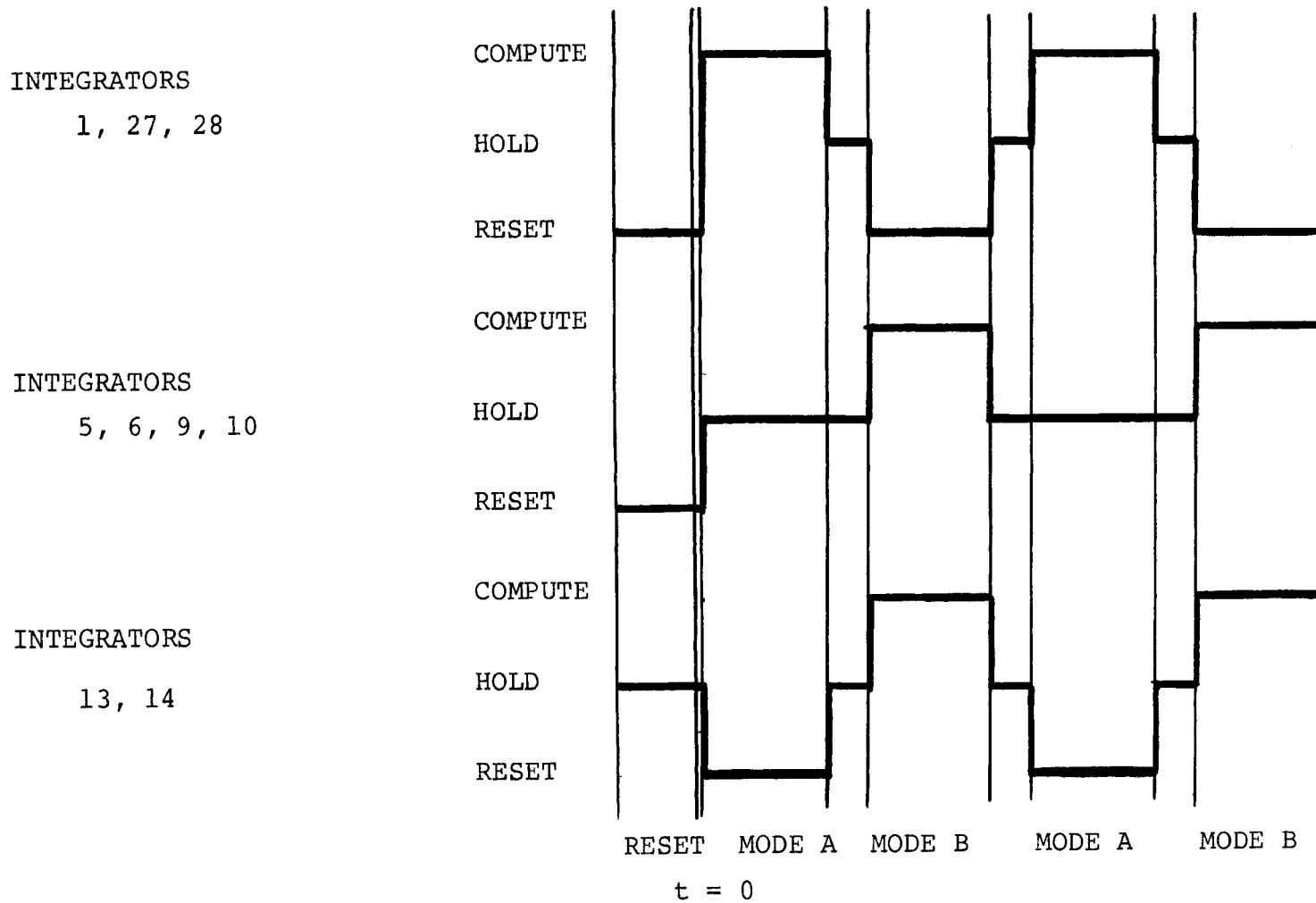RESET   MODE A   MODE B   MODE A   MODE B

$t = 0$

Figure 6.   Iterative Operation Switching
Diagram

mode, however the phase relationship between β and $\cos\psi$ could not be maintained unless the flapping equation loop and the $\sin\psi$, $\cos\psi$ loop were switching in the same manner. The method used by the author also makes $\sin\psi$ and $\cos\psi$ a true constant during the radial iteration as opposed to an assumed constant as $\sin\psi$ and $\cos\psi$ traverse a small angle.

In summary, the analysis presented on the preceding equations is limited by the following conditions:

1) The induced velocity through the rotor disc is assumed to be constant. This assumption has been shown to be reasonable for calculating performance of a rotor operation at tip-speed ratios greater than 0.10 but does result in error in computing blade motion, especially in the b_1 flapping coefficient. Certain vibration phenomena of helicopters in the transitional flight regime between hover and thirty miles per hour are attributable to the dissymetry of inflow in this region.

2) The assumption of uniform radial inflow is strengthened where twisted blades are used as in this simulation because the blade twist tends to give a uniform radial inflow. As flight speed is increased the

major portion of the rotor inflow is due
to the $V\sin\alpha_t$ component, rather than from
induced velocity. $V\sin\alpha_t$ is uniformly dis-
tributed across the rotor disc. This
assumption is not precise enough if the
simulation is extended to vibration analysis.

3) The radial component (third dimension) of
   the resultant air velocity at the blade
   elements has been neglected but all authors
   state that the effect of radial velocity
   increases the blade profile drag only
   slightly and has very little effect on rotor
   thrust.

4) Flapping angle, β, and the angle of inflow,
   ϕ, are assumed to be small angles . This
   assumption is valid for β if the rotor is of
   proper design and within its design range
   and especially where proper flap compensation
   is employed. The assumption is valid for ϕ
   for most ranges of helicopter operations but
   may lead to significant errors where the
   inflow is large, such as in steep rates of
   climb or descent, in which case a large
   vertical velocity is added to the rotor inflow
   component of U_p. The use of an electronic
   resolver for the solution of ϕ will solve

this problem.

5) The assumption is made that the reversed-
   flow region is negligible. It must be
   realized that this region increases with
   the tip-speed ratio and does contribute
   a decrease in overall rotor thrust and has
   an effect on the higher harmonics. Within
   the range of the 100 volt amplifiers of the
   SD 40/80, the effect is negligible.

6) The assumption is made that the blade is
   hinged on the axis of rotation. This is
   valid for a semi-rigid rotor. For an
   articulated rotor, flapping-hinge offset
   may be neglected in performance estimates
   but must be taken into account in stability
   and control analyses.

7) The lift-curve slope is assumed constant,
   the profile-drag coefficient is neglected
   as negligible within the amplifier range
   of the computer and blade stall is not
   modeled in the program. In a model of a high
   speed helicopter with a large power source
   and low fuselage profile drag, the resulting
   high tip speed ratios could result in a
   retreating blade stall and/or compressibility

at the tip of the advancing blade. The
result would be a rapid increase in blade
profile drag with a decrease in lift. The
simulation presented here would then result
in very optimistic performance predictions.
The existing program can easily be extended
to incorporate the blade stall and drag
component of thrust if high tip speed ratios
are to be simulated.

8) The rotor blade is assumed to be rigid
   in all directions. The effect of torsional
   and bending moments has been neglected. These
   deformations are small for normal blades
   when considering blade motion and rotor per-
   formance but become important in vibration
   analyses and control-force studies. Torsional
   deflections are also important in stability
   calculations.

9) The tip-loss assumption is sufficiently valid
   for this analysis but not for an extension to
   blade stress analyses.

10) A tapered blade can not be simulated in this
    analyses, however present day rotor blades
    are virtually all untapered.

CHAPTER IV

ANALYSIS OF DATA

The rotor blade simulated in this study was the
rotor blade for the Bell UH1D or UH1H model helicopter.
The UH1 employs a semi-rigid rotor head with two blades
rigidly joined to the rotor hub. The hub is gimbal
mounted to the rotor mast and consequently the blade
is free to flap up and down about a hinged axis whose
center is located at the center of the rotor mast. The
simulation was not a valid simulation of the UH1, as such,
partly because of the absence of the second blade which
contributes lifting moment opposing the lifting moment
of the opposite blade due to the rigid mounting to the
hub. The inertial forces of the opposing blade were
also not taken into account. Modeling of the single
blade, nevertheless, served the purposes of this study
and can be analagous to a single hinged blade of an
articulated rotor head with no hinge offset. The blade
airfoil designation is the NACA 0012 symmetrical air
foil and the coefficient of lift curve slope was approxi-
mated for the NACA 0012. Blade mass, length, chord and
twist for the UH1 blade were used. The blade is a
rectangular blade with constant chord length along the
blade radius (untapered). Since the blade twist starts
at r = 7.5 feet and the area of negative lift discussed

earlier is ignored, r_0 is taken at r = 7.5 feet. Lift
forces near the hub are small at moderate velocities.
Blade length is 24 feet, however, in order to take
into account tip losses, the generation of the radius
on integrator number 1 was integrated from 7.5 feet to
23 feet considering the large decrease in lift which
would occur near the tip. Tip losses normally reduce
the effective radius to 0.97R. A comparator was used on
integrator number 1 to prevent circuit overload during
switching time adjustments. Air density for standard
conditions at sea level was used since helicopter
operations are normally conducted at low altitude.

Data presented in this study is for a velocity of
50 miles per hour which is representative of blade
flapping in forward flight. At about this tip speed ratio
the constant induced velocity assumption becomes valid
and there exists no reverse flow region. Switching times
used in mode A and B were 26 milliseconds in each mode
with a 5 millisecond hold between each mode allowing for
a 4 millisecond overlap between modes. This gave a 62
millisecond iteration. The blade azimuth compute cycle
and flapping compute cycle was run at a compute time of
one tenth real time or 3.5 radians per second of azimuth
compute time since real time for the subject helicopter
is approximately 35 radians per second. The resultant
number of radial integrations per cycle was 66 integra-
tions per cycle of azimuth or one radial integration

every 5.45 degrees of azimuth. The computer thus com-
pleted one cycle of azimuth every 4.2 seconds. Note
that the azimuth and flapping loops are only in compute
for 26/62 of the total switching cycle times and are
holding for the remainder of the time.

Figure 7a represents the steady state flapping
angle β of the rotor blade at 50 miles per hour. The
flapping angle amplitude is approximately 0.20 radians
up and 0.12 radians down indicating a coning angle of
approximately 0.04 radians or 0.87 degrees. The phase
relationship of β with $\cos\psi$ was determined to be slightly
lagging $\cos\psi$ indicating that the flapping is not a
pure $a_o - a_1 \cos\psi$ flapping. Figure 7a shows the peak
flapping to the left of the nose of the helicopter. It
was stated earlier that sideward flapping b_1 is indepen-
dent of blade mass. The exciting forces for b_1 motion
are, however, proportional to the coning angle which is
proportional to the mass of the blade. Oscillation
amplitude of a resonant system with damping is propor-
tional to the magnitude of excitation. Consequently, as
the blade mass increases infinitely, coning decreases to
zero and b_1 disappears since its exciting force disappears.
Figure 7b illustrates β where the inertial forces have
been increased by a factor of 100. The magnitude of
flapping has been reduced to +0.0013 radians with no
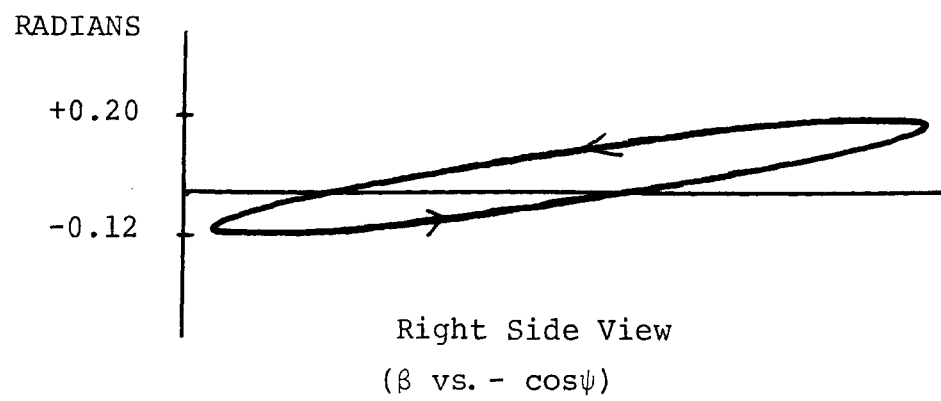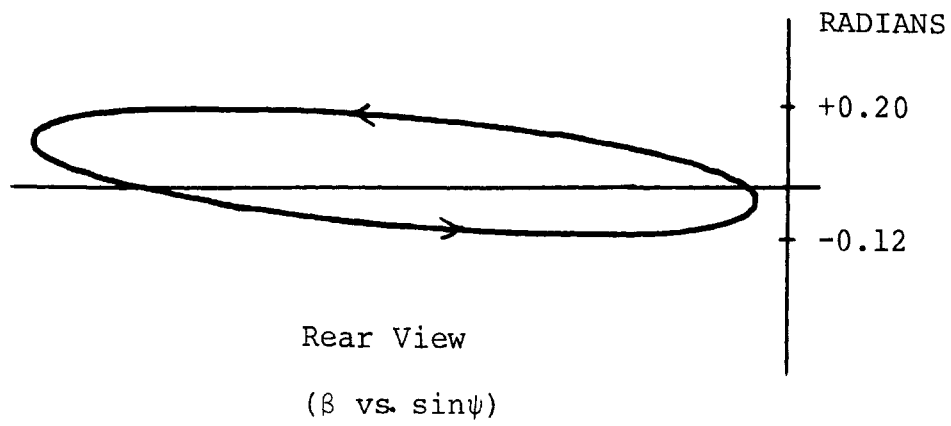detectable coning angle and a resulting almost pure a_1

Rear View

(β vs. sinψ)

RADIANS

+0.20

-0.12

RADIANS

+0.20

-0.12

Right Side View

(β vs. - cosψ)

Figure 7a. Normal Inertia Tip Path Plane

RADIANS

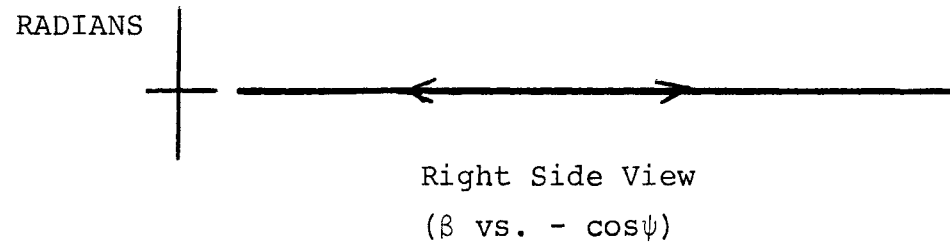Rear View

(β vs. sinψ)

RADIANS

Right Side View

(β vs. - cosψ)
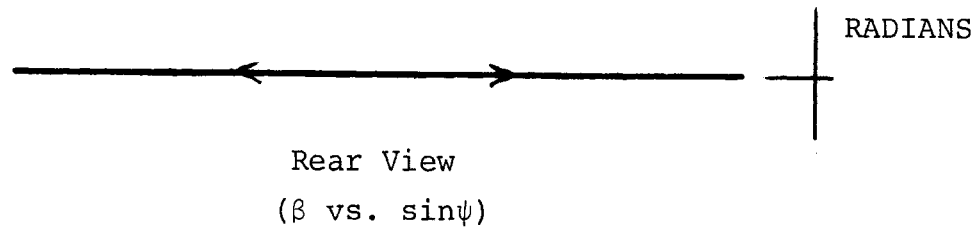
Figure 7b. One Hundred Times Normal Inertia
            Tip Path Plane

RADIANS

+0.05

−0.03

Rear View

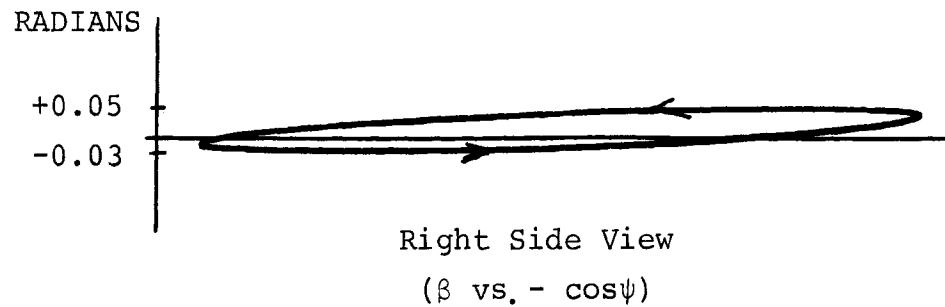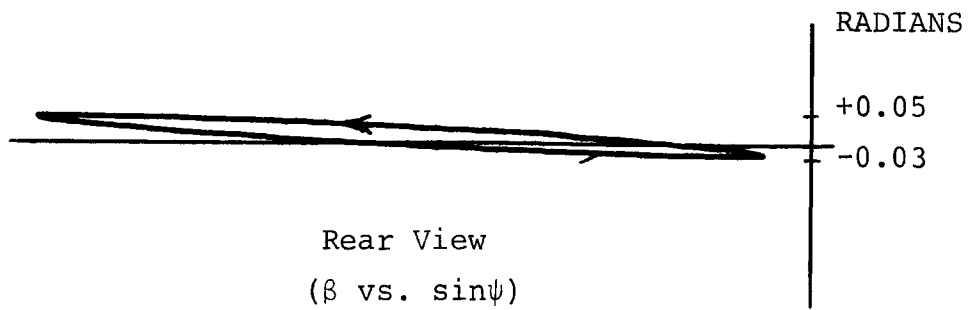(β vs. $\sin\psi$)

RADIANS

+0.05

−0.03

Right Side View

(β vs. $-\cos\psi$)

Figure 7c.   Ten Times Normal Inertia Tip Path Plane

RADIANS
+0.40

−0.05

Rear View

(β vs. sinψ)

RADIANS

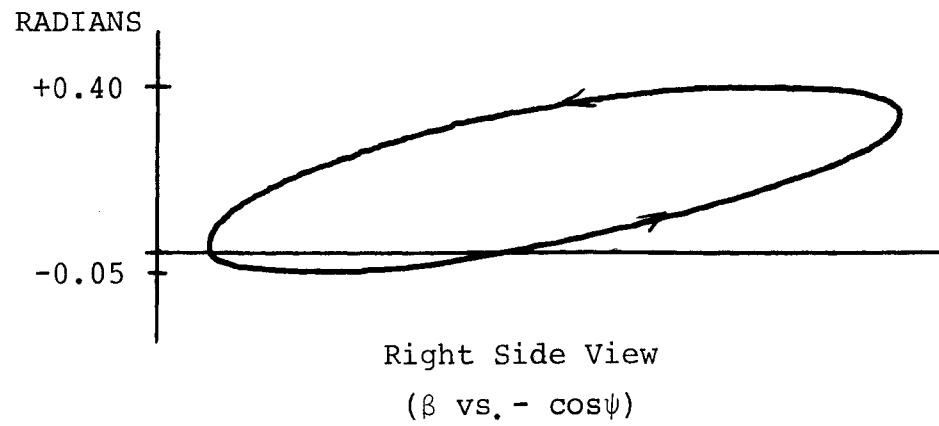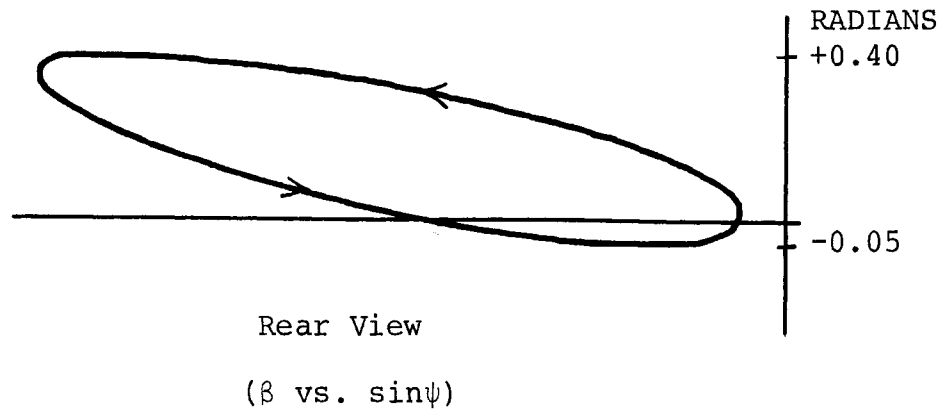+0.40

−0.05

Right Side View

(β vs. − cosψ)

Figure 7d. One Tenth Normal Inertia Tip Path Plane

$\cos\psi$ flapping motion. The phase relationship with $\cos\psi$ is in phase as determined from other data. Figure 7c shows the flapping magnitude and rotor tilt for an intermediate value of ten times normal inertia.

Conversely, a decrease in inertial forces resulting from a lighter blade should yield larger flapping, larger coning angle, greater sideward tilt (b_1), and higher harmonic flapping. Figure 7d shows flapping magnitude for one tenth normal inertia. The resulting flapping magnitude is approximately 0.40 radians positive and 0.05 radians negative for a coning angle of approximately 0.22 radians. The phase relationship of β with $\cos\psi$ has moved substantially so that the peak angle of flapping is farther to the left of the nose of the aircraft yielding a more definite sideward tilt (b_1) and possible higher harmonics in addition to the increased coning angle. As β increases out of the small angle range, accuracy decreases because of the small angle assumption. The results, however, indicate agreement with the theory of flapping expressed in Gessow and Myers which is also derived from experimental and wind tunnel studies.

The variation in the simulation is made at this point to incorporate a flapping compensator into the hinge of the rotor blade. Figure 8a depicts a hinged blade with what Mil (1967, p. 94) calls a turned hinge.
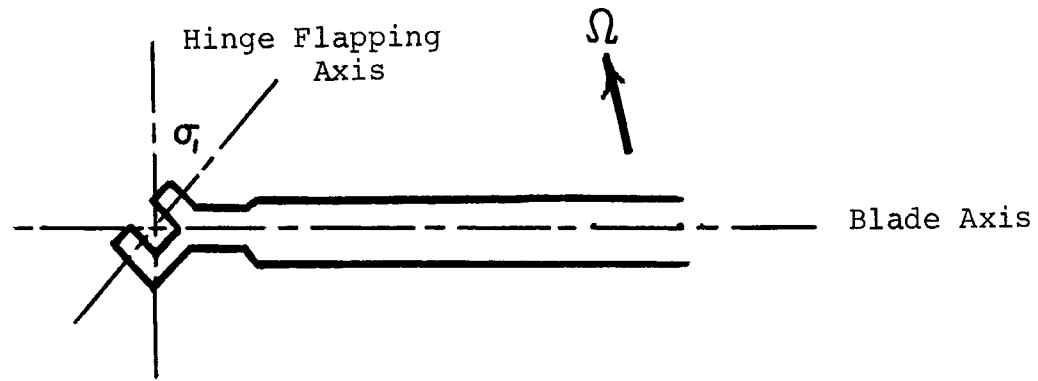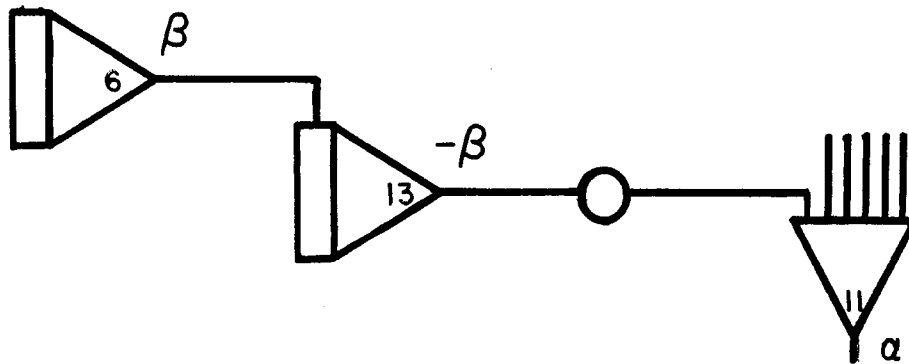
Figure 8a.   Hinged Blade with Turned Hinge

Figure 8b.   Analog Circuit for Flap Compensator

It can be seen from figure 8a that when the blade flaps
up, the angle of attack is simultaneously decreased. The
opposite case is true when the blade flaps down. The result
is a damping of rotor oscillation due to differential lift,
provided that the angle of the compensator is not excessive.
The same result can be achieved on a semi-rigid rotor where
push-pull control rods link the swash plate either directly
or through a stabilizer bar with the pitch change arms on
the forward portion of the rotor blade. When the blade
flaps up, the swashplate connections pull down on the pitch
change arms thus reducing the blade pitch in the manner of
the turned hinge. The opposite effect results when the
blade flaps down.

The flap compensator for a zero cyclic feathering
condition was simulated on the analog by feeding back an
inverted portion of the flapping angle to the angle of
attack summer. The circuit used for the simulation is
illustrated in figure 8b. Because of lack of amplifiers,
the remaining integrator from the module containing the
track integrator was used to track $-\beta$ and feed it into
summer number 11 through a scaling potentiometer. An
excessive feedback greatly upsets the system but a small
value of feedback has a substantial damping effect shown
relative to the control axis in figure 9. The magnitude
of the feedback potentiometer would be proportional to
the angle of turn of the flapping hinge or the length of

RADIANS

+0.05
−0.03

Rear View

(β vs. sin ψ)

RADIANS

+0.05
−0.03

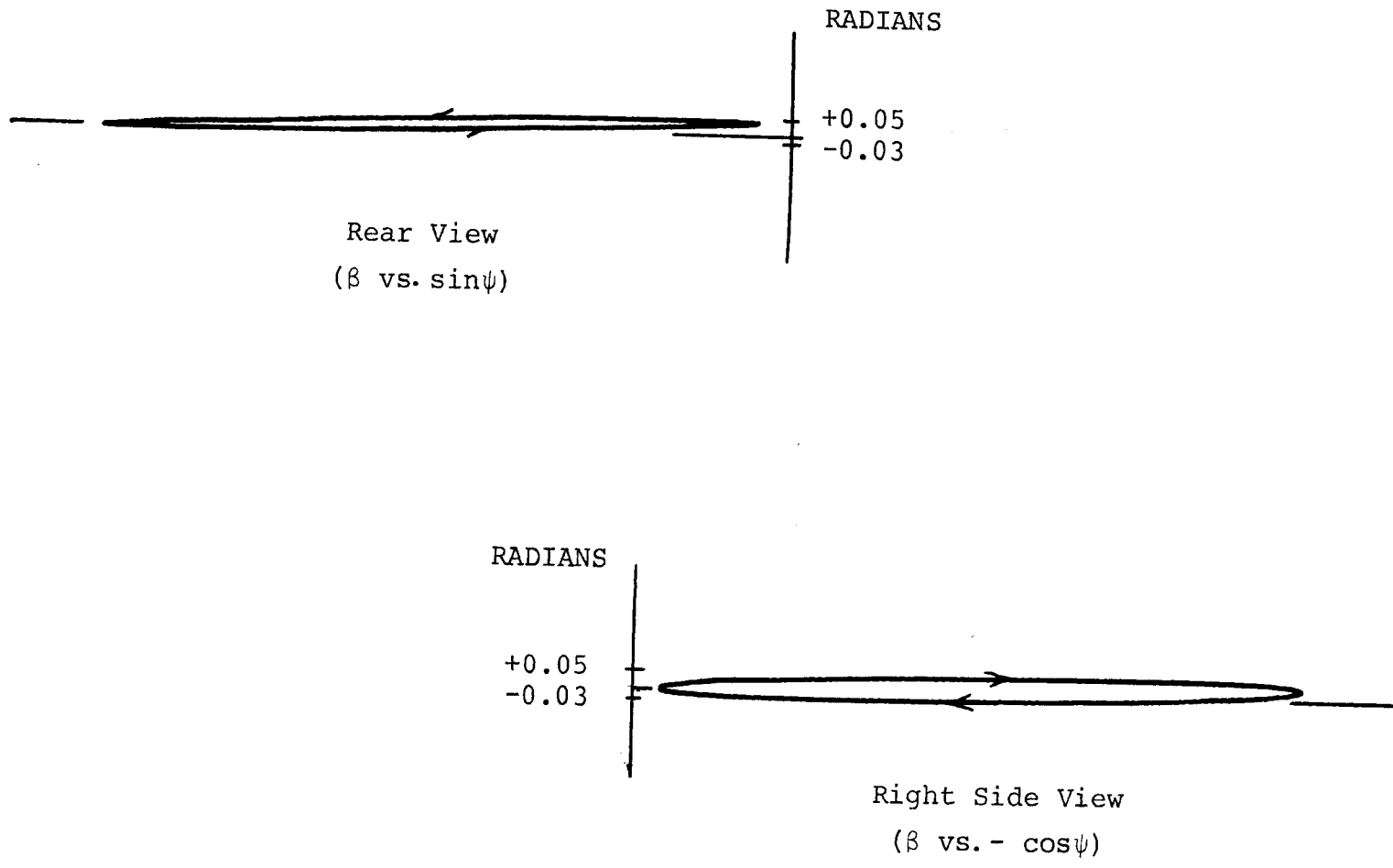Right Side View

(β vs. − cos ψ)

Figure 9. Normal Inertia, with Flap Compensation, Tip Path
Plane

the pitch change arm on a semi-rigid rotor. Mil (1967, p. 94) states that the angle of change of pitch, Φ, due to flapping compensation, varies in accordance with the law $\Phi = \theta_o - \beta \tan\sigma_1$ and presents an interesting discussion of the effects of the turned hinge on rotor phase relationships under given conditions. These conditions were not simulated or analyzed in this study but could be analyzed in an extended study.

For academic illustration of the effect of control changes on the flapping of the rotor see figures 10a thru 10c. Flapping in the above case represents flapping due to collective and cyclic pitch changes in addition to pure differential lift induced flapping and, except for 10a, is not flapping with respect to the control axis. When cyclic pitch is added through swashplate tilt, the control axis tilts with the swashplate.

The rotor of figure 10 a at plot time zero has a 50 mile per hour forward velocity with a flat collective pitch input. Consequently there is a negative angle of attack at the outer radius of the rotor and a consequent forward and left tilt of the rotor. As the blade advances to the retreating side of the disc, collective pitch is added, yielding a positive lift and the resultant rearward tilt of the rotor disc due to flapping until steady state is reached. It should be noted that induced velocity was not varied when collective pitch was added but the predominant portion of the inflow comes from the forward

Flapping With Collective Pitch Added

RADIANS

Right Side View
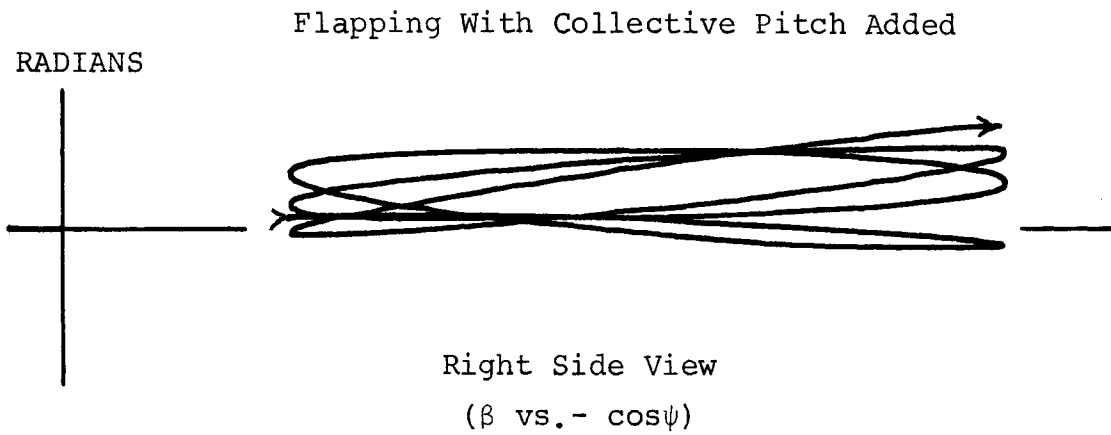
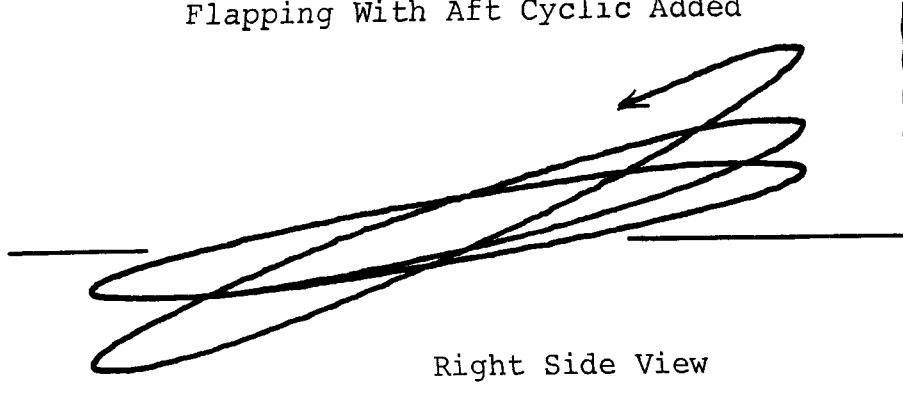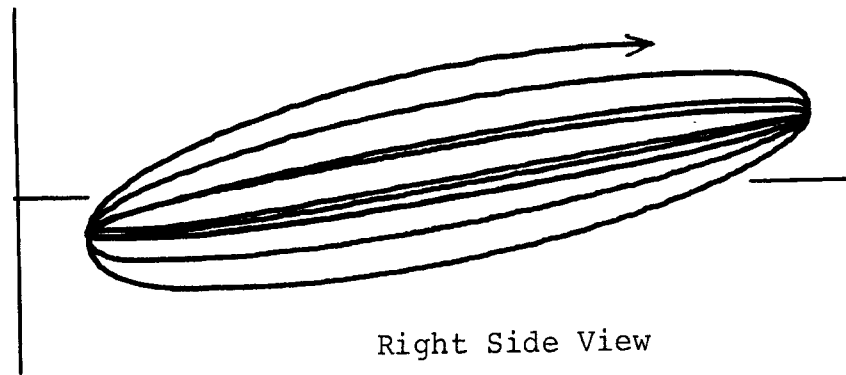$(\beta$ vs.$-\cos\psi)$

Figure 10a. Tip Path Plane With Transient
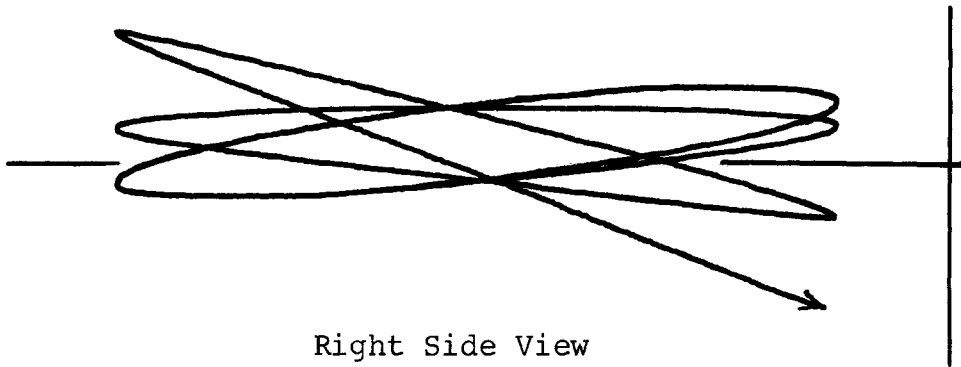Collective Pitch

Flapping With Aft Cyclic Added

Right Side View

Flapping With Left Cyclic Added

Right Side View

Figure 10b. Tip Path Plane With Transient Cyclic Pitch

Flapping With Forward Cyclic Added

Right Side View

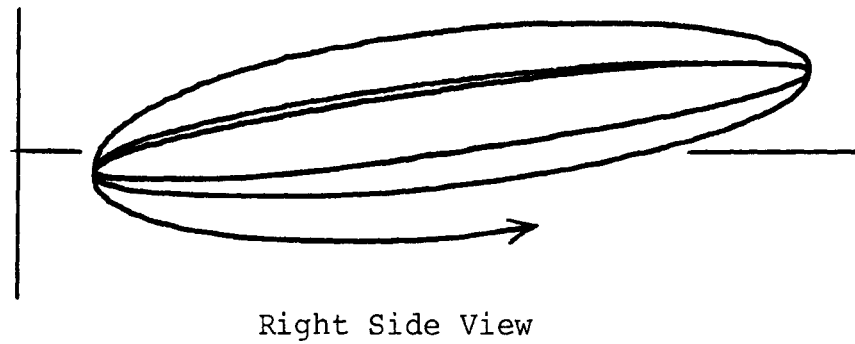Flapping With Right Cyclic Added

Right Side View

Figure 10c. Tip Path Plane With Transient Cyclic Pitch

velocity through the tilted rotor at 50 miles per hour.
This illustrates the transient effect of an increase in
collective pitch on the tilt of the rotor tip path plane
and thrust vector. This phenomenon during take-off and
landing, when collective pitch is suddenly added, has
been called "zooming" and is described by Gessow and
Myers (1967) as an undesirable tendency. This author
believes that on the contrary this "zooming" effect
can be put to good use by the pilot when flying a heavily
loaded helicopter in and out of confined areas. The
"zooming" somewhat extends the aft cyclic control which
is normally decreased in a single main rotor helicopter
where loads are carried forward of the rotor shaft.

In order to gain an insight into the quantitative
aerodynamic changes taking place during a steady state
cycle of azimuth traverse of the rotor blade, figure 11a
thru 11d illustrate rough plots of some of the parameters
evaluated by the computer during simulation. Phase
relationships with the azimuth angle could not be depicted
on the single track recorder utilized for this data and
the slowness of the plotter in following the rapid radial
integrations of the computer substantially reduces the
accuracy of the plot radial envelopes. Values for the
actual radial envelope boundaries are shown on the plot
ordinate and one cycle of azimuth rotation is marked on
each plot abscissa. More accurate data illustrating the
parameter plots opposite the cosine of the azimuth angle ψ

recorded on dual track lined recording paper are
available in departmental files. Nevertheless, the plots
presented here serve the stated purpose.

The data for figures 11a thru 11d are for the normal
blade inertia condition without flap compensation. The
induced velocity at 50 miles per hour was estimated from
Wood & Hermes (1969, p. 13). Since induced velocity is
considered constant, errors in magnitude of induced velocity
would be partly compensated for by a requirement for a
changed collective pitch in order to maintain the desired
lift equal to an assumed weight of the helicopter. Recall
that $\phi = \tan^{-1} \frac{U_p}{U_T}$ which affects the angle of attack α but
the effect of U_p^2 on W^2 is small due to the large magnitude
of U_T^2 in comparison with U_p^2, where $W^2 = U_p^2 + U_T^2$. It can
be seen from the data that the small angle assumptions
used in the study are valid. The angle of tilt of the
control axis or swash plate, α_t, was taken from data in
Schramm (1970, p. 236) where the pitch angle of the fuselage
at the given velocity plus the aft pitch of the fuselage at
a hover represented the angle of pitch of the swashplate in
forward flight at 50 mph. At a hover, the tilt of the
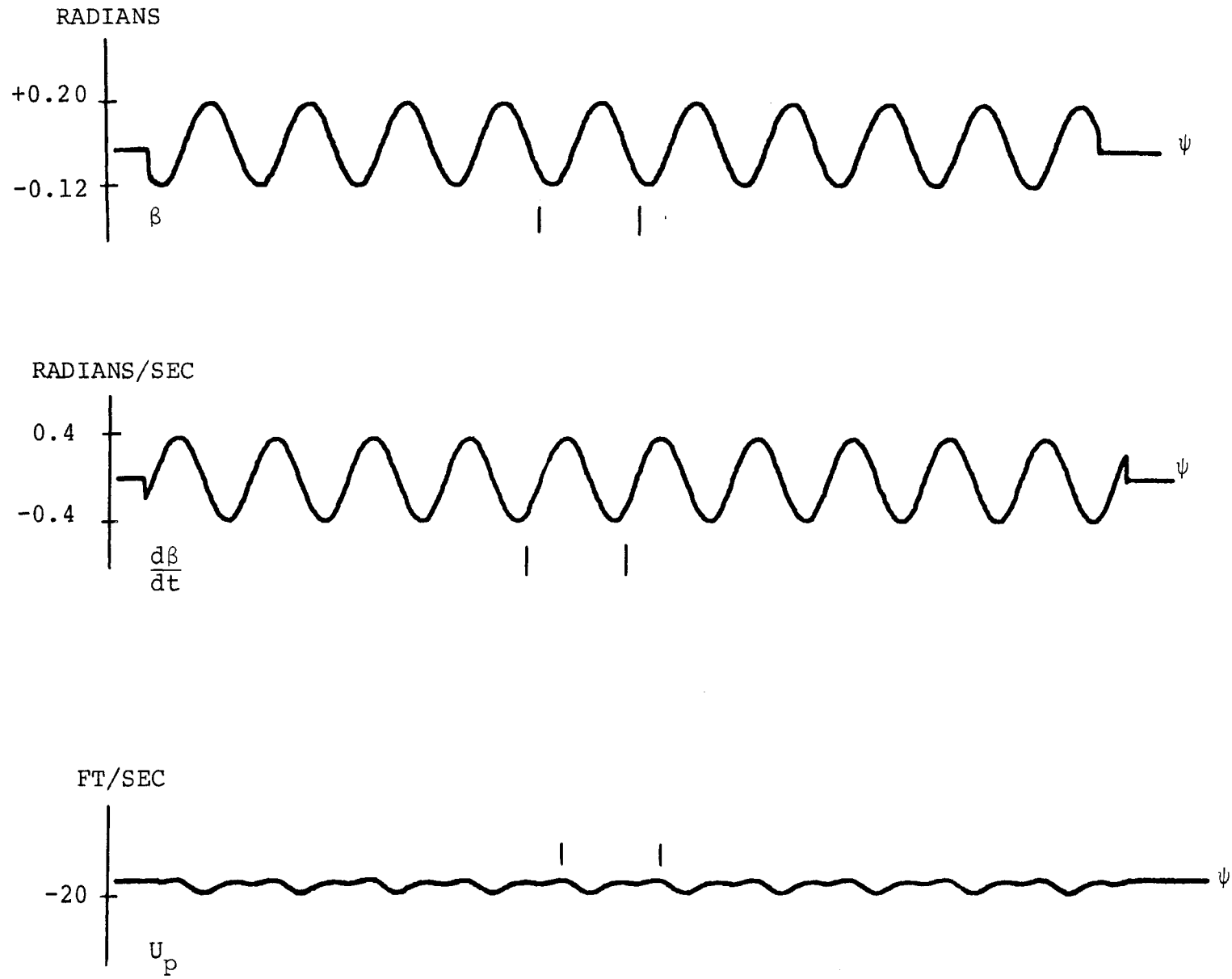swashplate and rotor hub is zero.
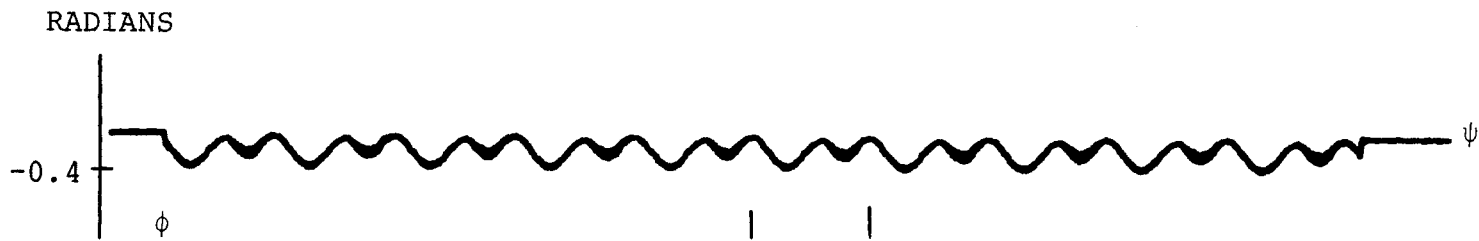
Figure 11a. Steady State Parameter Plots

Figure 11b.   Steady State Parameter Plots
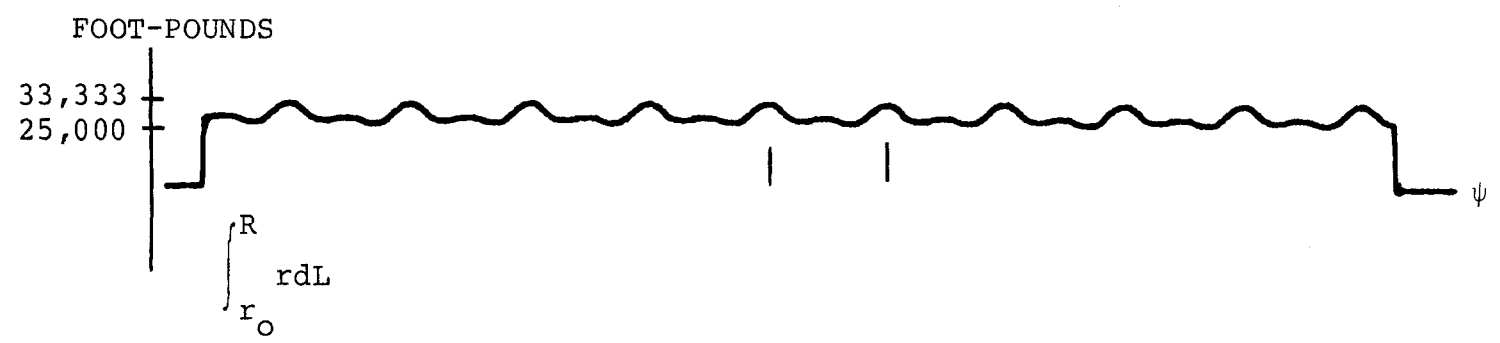
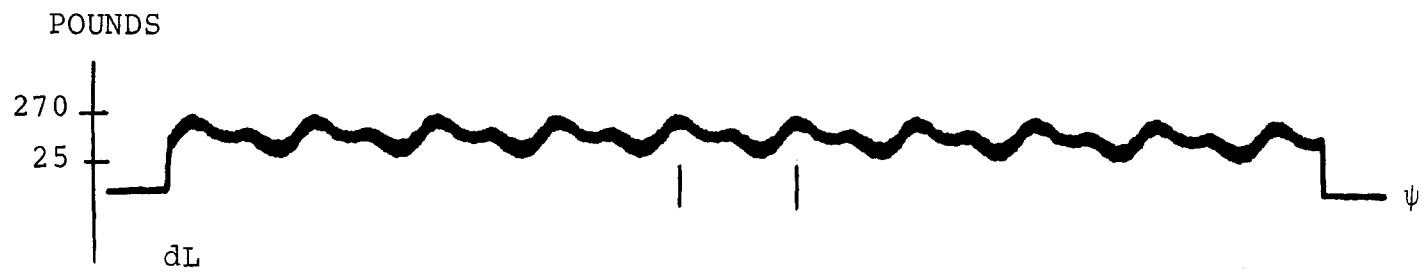Figure 11c.   Steady State Parameter Plots

Figure 11d. Steady State Parameter Plots

CHAPTER V

DISCUSSION

It is felt that a useful and realistic simulation
of a helicopter main rotor can be accomplished within
the constraints of the Systron Donner 40/80 electronic
analyzer. The resulting flapping angle magnitudes and
phase relationships conform with well established
theoretical and experimental expectations. The analog
computation permits constant visual observation of such
parameters as flapping angles, flapping velocities,
resultant velocity, angle of inflow through the main rotor,
resultant angle of attack, coefficient of lift, radial
distribution of lift and lifting moment.

These parameters can be observed over the length
of rotor radius and throughout the azimuth of traverse.
Very fast synchronized recording equipment is necessary
to gain full value of these observations. Such para-
meters as lift distribution along the rotor radius can
only be observed on an oscilloscope trace due to the
rapid radial integration and varying magnitudes around the
rotor azimuth. The effect of blade weight, radial length,
and rotational velocity on the inertial forces and the
resultant flapping magnitudes can be evaluated at varying
forward airspeeds. A preliminary blade design for an

untapered blade can be simulated and analyzed within the constraints of the program and computer components.

CHAPTER VI

RECOMMENDATIONS

It is recommended that with the acquisition of
additional components a two bladed semi-rigid rotor be
modeled and analyzed for the effect of the opposing
blade, taking into consideration flapping compensation.
It is felt that with three additional integrator modules,
two for track and store and one for a second $\sin\psi$, $\cos\psi$
loop, a second blade could be simulated using 4 electronic
switches to switch the first and second blade into and
out of the lift moment integral evaluating circuit, in
succession. This would necessitate a further revision of
the digital logic rep-op drive program with direct logic
voltages applied to the individual computer modules, not
through the C-R-H busses, for successive switching.

It is further recommended that an analysis of the
effect of flapping compensation on flapping magnitude
and phase relationships be made as stated earlier.

NOMENCLATURE

a   slope of lift coefficient, units/radian

a_o coning angle of rotor blade span axis, radians

a_1 Fourier coefficient for longitudinal blade flapping, radians

b_1 Fourier coefficient for lateral blade flapping, radians

c   rotor blade chord, ft.

C_L blade element lift coefficient, dimensionless

C_D blade element drag coefficient, dimensionless

dL   blade element lift, pounds

dr   length of element of blade radius, feet

dT   blade element thrust, pounds

I   moment of inertia about flapping hinge, slug-ft^2

m   blade element mass, pounds/foot

r   blade radius, feet

r_o blade radius at lower boundary of integration, feet

R   radius of blade tip, feet

U_p velocity component perpendicular to swash plate or parallel to control axis, feet/second

U_T velocity component parallel to swash plate or perpendicular to control axis, feet/second

W   resultant velocity of relative wind, feet/second

Greek Symbols

α resultant blade element angle of attack, radians

α_t angle of tilt of control axis from perpendicular or tilt of swashplate from horizontal, radians

β flapping angle of rotor blade, radians

γ Lock number

ψ azimuth of blade rotation from aft of rotor disc, radians

σ_1 angle of turn of flapping hinge, radians

θ_o angle of collective pitch, radians

θ_1 angle of lateral cyclic pitch, radians

θ_2 angle of longitudinal cyclic pitch, radians

θ_r blade twist per unit length of radius, radians/foot

θ_t total blade twist at radius r, radians

ρ atmospheric density, slugs/ft.^{3}

Ω rate of blade rotation, radians/sec.

ϕ angle of inflow through rotor disc, radians

Φ angle of change of pitch due to flapping compensation, radians

BIBLIOGRAPHY

Gessow, Alfred, and Myers, Garry C., Jr. Aerodynamics
of the Helicopter. New York: Frederick Ungar
Publishing Co., 1967.

Gilliland, Maxwell C. Handbook of Analog Computation.
Concord, California: Systron Donner Corporation,
1967.

Hurt, H.H., Jr. Aerodynamics for Naval Aviators. Washington
U.S. Navy, Revised 1965.

Hohenemser, K.H. "Analysis of the Vertical Flight
Dynamic Characteristics of the Lifting Rotor With
Floating Hub and Offset Coning Hinges," Journal of
the American Helicopter Society, III, 4,(October,
1958), 20-34.

Jones, Jeffrey P. "Calculation of Helicopter Blade
Loading by Means of an Analogue Computer," Technique
de Calcul Analogique et Numerique en Aeronautique,
(September, 1963), 122-131.

Jones, Jeffrey P. "The Use of an Analogue Computer to
Calculate Rotor Blade Motion," Journal of the
American Helicopter Society, IX, 2, (April, 1964)
25-31.

Jones, Jeffrey P.   "The Helicopter Rotor,"   The Aero-
nautical Journal of the Royal Aeronautical
Society, LXXIV, 719, (November, 1970), 861-872.

MacNeal, R.H.   "Direct Analog Method of Analysis of the
Vertical Flight Dynamic Characteristics of the
Lifting Rotor With Floating Hub,"   Journal of the
American Helicopter Society, III, 4, (October, 1958),
35-49.

McCormick, Barnes W., Jr.   Aerodynamics of V/STOL Flight.
New York: Academic Press, 1967.

Mil', M.L., et al.   Helicopters - Calculation and Design,
Volume I. Aerodynamics, Moscow: "Mashinostroyeniye"
Publishing House, 1966. (NASA Technical Translation).

Mil', M.L., et al.   Helicopters - Calculation and Design,
Volume II. Vibrations and Dynamic Stability.   Moscow:
"Mashinostroyeniye" Publishing House, 1967. (NASA
Technical Translation).

Miller, R.H. "On the Computation of Airloads Acting on
Rotor Blades in Forward Flight", Journal of the
American Helicopter Society, VII, 5, (April, 1962),
56-66.

Miller, R.H. "Unsteady Airloads on Helicopter Rotor Blades,"
Journal of the Royal Aeronautical Society, LXVIII,
640, (April, 1964), 217-229.

Nikolsky, Alexander A. Helicopter Analysis. New York:
    John Wiley and Sons, Inc., 1951.

Payne, P.R. Helicopter Dynamics and Aerodynamics.
    London: Sir Isaac Pitman and Sons, Ltd., 1959.

Report prepared for the U.S. Army Electronics Laboratories,
    Fort Monmouth, N.J. Under Contract No. DA 28-043
    AMC-00498(E). The Simulation of Helicopter Motion
    and Avionics Systems, G.R. Bolton, E.E.L. Mitchell,
    I. Hay. Princeton: Electronic Associates, Inc.,
    1965.

Shapiro, Jacob. Principles of Helicopter Engineering. New
    York: McGraw Hill Book Co., Inc., 1956.

Schramm, Milton. "Real-Time Simulation of a Helicopter
    Rotor on an Analog Computer," Simulation, XIV,
    (May, 1970), 231-237.

Technical Report: ECOM 0387-F1 Prepared for U.S. Army
    Electronics Command, Fort Monmouth, N.J., Under
    Contract No. DAAB07-68-C-0387. Development of
    Hybrid Computer Programs for Simulation of the
    Cheyenne (Advanced Aerial Fire Support System),
    I. Hay, E.E.L. Mitchell. Princeton: Electronic
    Associates, Inc., 1969.

Technical Report: ECOM 0387-F2a Prepared for U.S. Army
    Electronics Command, Fort Monmouth, New Jersey,

Under Contract No. DAAB07-68-C-0387. Development
of Hybrid Computer Programs for Simulation of
Cobra,   E.B. Baker, I. Hay, E.E.L. Mitchell,
Princeton: Electronics Associates,Inc., 1969.

Technical Report: NAVTRADEVCEN 1205-1 Prepared for U.S.
Naval Training Device Center, Port Washington,
New York. Simulation of Helicopter and V/STOL
Aircraft. Volume I. Helicopter Analysis Report,
James R. Toler, Walter McIntyre, Merlin P. Coffee.
Falls Church, Virginia: Melpar Inc.,1963.

Technical Report: NAVTRADEVCEN 1205-4 Prepared for U.S.
Naval Training Device Center, Port Washington,
New York. Simulation of Helicopter and V/STOL
Aircraft. Volume IV. Helicopter Analysis Report,
R. Anthony. Falls Church, Virginia: Melpar Inc.,
1964.

Thomson, William T. Vibration Theory and Application.
Englewood Cliffs, N.J.: Prentice-Hall, Inc., 1965.

Velkoff, Henry R. Introduction to Helicopter Analysis
and Design. Unpublished text utilized by the author
at Ohio State University, Columbus, Ohio.

Volodkov, A.M., Livshits, G.L. "Dynamics of a Helicopter
After the Loss of a Portion of the Main Rotor and

Tail Rotor Blades," <u>Izdatel' Stvo Nauka</u>, (1968), 89-97. (in Russian).

Wood, E.R., Hermes, M.E. "Rotor Induced Velocities in Forward Flight by Momentum Theory," <u>AIAA Paper No. 69-224</u>, (February, 1969), 1-6.

Young, Raymond A. <u>Helicopter Engineering</u>. New York: The Ronald Press, Company, 1949.

VITA

Edward Charles Robinson, son of Mr. and Mrs. Charles Kimball Robinson, was born in Greenwich, New York on May 26, 1937.

He attended Troy High School in Troy, New York and was graduated in June, 1955. In July, 1955 he entered the United States Military Academy, West Point, New York and received his Bachelor of Science Degree in June of 1959. He was commissioned in the United States Army at that time and has served as a regular army officer since that time. He has served various tours of duty within the Continental United States as well as the Far East and Europe. He has attended numerous Army schools and is a Senior Army Aviator, qualified in single and multi-engine fixed wing and rotary wing aircraft. As of this writing, he has attained the rank of Major. He entered the University of Missouri-Rolla in January 1970 as a candidate for the degree of Master of Science in Aerospace Engineering.

He is married to the former Patricia Ann Jones of Troy, New York and is the father of three children.